



# *Concept and methodology of characterising infrared radiative performance of urban trees using tree crown spectroscopy*

Article

Accepted Version

Creative Commons: Attribution-Noncommercial-No Derivative Works 4.0

Deng, J., Pickles, B. J., Kavakopoulos, A., Blanusa, T., Halios, C. H., Smith, S. T. and Shao, L. (2019) Concept and methodology of characterising infrared radiative performance of urban trees using tree crown spectroscopy. *Building and Environment*, 157. pp. 380-390. ISSN 0360-1323 doi: <https://doi.org/10.1016/j.buildenv.2019.04.056> Available at <http://centaur.reading.ac.uk/83478/>

It is advisable to refer to the publisher's version if you intend to cite from the work. See [Guidance on citing](#).

To link to this article DOI: <http://dx.doi.org/10.1016/j.buildenv.2019.04.056>

Publisher: Elsevier

All outputs in CentAUR are protected by Intellectual Property Rights law, including copyright law. Copyright and IPR is retained by the creators or other copyright holders. Terms and conditions for use of this material are defined in the [End User Agreement](#).

[www.reading.ac.uk/centaur](http://www.reading.ac.uk/centaur)

## **CentAUR**

Central Archive at the University of Reading

Reading's research outputs online

1 Manuscript for *Building and Environment*

2

3 **Title: Concept and methodology of characterising infrared radiative performance of**  
4 **urban trees using tree crown spectroscopy**

5

6 Jie Deng<sup>1,\*</sup>, Brian J. Pickles<sup>2</sup>, Anestis Kavakopoulos<sup>1</sup>, Tijana Blanusa<sup>3</sup>, Christos H. Halios<sup>1</sup>,  
7 Stefan T. Smith<sup>1</sup> and Li Shao<sup>1</sup>

8

9

10 <sup>1</sup> School of Built Environment, University of Reading, Chancellor's Building, Whiteknights,  
11 Reading, RG6 6DF, UK.

12

13 <sup>2</sup> School of Biological Sciences, University of Reading, Harborne Building, Whiteknights,  
14 Reading RG6 6AS, UK.

15  <https://orcid.org/0000-0002-9809-6455>

16

17 <sup>3</sup> School of Agriculture, Policy and Development, Agriculture Building, University of  
18 Reading, Whiteknights, Reading, RG6 6BZ, UK.

19

20 *\*Author for correspondence:*

21 *Jie Deng*

22 *Tel: +44 (0) 118 378 5835*

23

24 *Emails: j.deng@reading.ac.uk; deng-jie2@163.com (J. Deng)*

25

26 **Abstract**

27 Urban trees play an important role in cooling urban microclimates and regulating outdoor  
28 thermal comfort. To better understand their contribution to these processes, it is crucial to  
29 elucidate urban trees' radiative thermal performance, especially in the infrared (IR) region  
30 (approximately 50% of solar radiation). Yet, owing to significant conceptual and  
31 methodological challenges, studies on the radiative performance of trees have mainly  
32 focused on individual leaves rather than crown-level characteristics. Here we applied a novel  
33 conceptual and methodological framework to characterise the crown-level IR radiative  
34 performance of 10 lime trees (*Tilia cordata*), a common urban tree in the UK and Europe. Our  
35 results show that reflected and transmitted solar energy from leaves is dominated (>70%) by  
36 IR radiation. At the leaf level, transmission and reflection spectra are similar between trees  
37 (differences typically < 10% in IR region), including those under significantly different urban  
38 stress conditions. However, at the crown-level, substantial variations in IR transfectance  
39 spectra (maximum difference > 40% in IR region) were found between trees. These variations  
40 were largely due to crown structural differences (leaf number, density, angles), rather than  
41 leaf solar interaction character (leaf-level transmittance or reflectance, leaf colour). Crown  
42 transfectance measured from the four cardinal directions was significantly different in the IR  
43 region (maximum differences circa 30%), and changed substantially with solar time. Hence,  
44 a tree's surroundings received very different, and time dependent, levels of solar IR radiation.  
45 These findings have significant implications for species selection and control of  
46 environmental stress factors in urban microclimates.

47

48 **Keywords:** Infrared radiative performance; Transfectance spectra; Tree crown spectroscopy;  
49 Urban cooling; Urban microclimate; Urban trees

50

## 51 **1 Introduction**

52 Urban green spaces and trees have substantial benefits for people's health, thermal  
53 comfort, pollution and noise reduction, sustainable urban drainage, and carbon  
54 sequestration [1]. In particular, trees and green spaces offer significant cooling benefits  
55 through canopy absorption, reflection, and transpiration, thereby helping to mitigate  
56 microclimatic environment in cities and towns and regulate outdoor thermal comfort [2–7].  
57 Surface temperatures of trees and green spaces are typically 10-20 °C lower than those of  
58 full sun exposed ground and built surfaces [2, 7–10], leading to a significant reduction of  
59 radiant temperatures. Areas shaded by trees can be cooler than tree surfaces [11]. Air  
60 temperature reductions are smaller, typically up to 3.5 °C below the tree canopy [2, 7, 12,  
61 13]. Trees are also effective, though to a lesser extent, in ameliorating urban heat island  
62 (UHI) [14,15]. In the sense of regulating the outdoor environment, urban trees will help to  
63 mitigate extreme heat stress through cooling, and anthropogenic global warming through  
64 carbon sequestration [16] as well as reduced cooling energy demand [17]. Among the many  
65 climate change projections of the UKCP09 [18], the ones that have the greatest impact on  
66 design of the built environment are increasing temperatures and increasing aridity, resulting  
67 in hotter and drier summers. The global average temperature rise will be accompanied by  
68 more frequent and intense extreme weather events, e.g. heatwaves, such as that of 2003,  
69 which resulted in over 2000 extra deaths in the UK and circa 35,000 across Europe [19]. By  
70 the end of the century a heatwave could be 10 °C hotter than it is today in the UK [18]. This  
71 is intensified by the UHI effect, which could lead to exceptional heatwave periods [20, 21].

72  
73 To maximize the effect of trees on cooling microclimates in hot and arid summer conditions,  
74 research has focused on exploring thermal performance differences among various tree  
75 species, and providing tree planting guidelines for policy makers and urban planners, with  
76 the aim of developing resilient and resourceful cities [2–7, 12, 22, 23]. Tree species differ  
77 significantly in their ability to i) reduce air and surface temperature, and ii) increase relative  
78 humidity [7]. Zheng et al. [2] assumed that different tree morphology and characteristics  
79 among various tree species led to large differences in trees' cooling performance. They  
80 investigated three physiological indices (leaf transpiration rate, leaf surface temperature,  
81 and leaf reflectance) as well as seven microclimatic parameters (solar radiation, long wave  
82 radiation, mean radiant temperature, ground surface temperature, air temperature, relative  
83 humidity, wind speed) characterising four common tree species in Guangzhou, China (a  
84 subtropical region). Irmak et al. [4] concluded that surface temperatures of different tree  
85 species varied considerably and that the “sky-view factor” had a significant effect on tree

86 surface temperatures, by assessing thermal effects of 15 different tree species (4  
87 coniferous and 11 deciduous) located in the northeastern part of Turkey. The sky-view  
88 factor measures the visibility of the sky from a given point, with a value between 0 and 1,  
89 where a value of 1 means that the sky is completely visible from that point. A study of 10  
90 common urban tree species in Basel, Switzerland, indicated that tree species differed by up  
91 to 9 °C in their canopy surface temperatures [10]. In view of this, choosing the right tree  
92 species for urban planting schemes is critical for maximizing their cooling potential.  
93 Morakinyo et al. [22] indicated that leaf-area index (LAI) was the main driver of the  
94 observed benefits, followed by trunk height, tree height, and crown diameter via a  
95 simulation study, taking into account the 8 most common tree species in Hong Kong. Tree  
96 species with higher LAI provided significantly more cooling than the other species, and  
97 surface temperature reduction was positively correlated with LAI [24]. Faster growing  
98 species showed higher LAI and higher stomatal conductivity and so provided more cooling  
99 benefits [25]. Lindén et al. [26] showed that transpiration-induced cooling from trees was an  
100 important driver of intra-urban differences in Mainz, Germany. It is reckoned by Shahidan et  
101 al. [27] that shading from trees and evapotranspiration are the prime factors that contribute  
102 to decreased air temperature. A similar viewpoint was presented by Gillner et al. [7], who  
103 argued that trees showing both a high leaf-area density and a high rate of transpiration  
104 were more effective in cooling air temperatures. The shading effect of trees is closely  
105 related to LAI and some work has already focused on modelling or measuring the shading  
106 effect [6, 28–33]. However, within this body of work, it seems that the mechanism of the  
107 shading effect has not yet been elucidated (e.g. from the perspective of radiative  
108 performance of trees) in terms of reflectance and transmittance.

109  
110 To a large extent, urban tree planting guidelines are proposed according to trees' thermal  
111 performance. Some research has proposed useful guidelines based on a simplification of  
112 trees' physical characteristics or using a statistical method. Zhao et al. [3] explored optimal  
113 tree arrangement for both individual households and residential neighborhoods in a hot arid  
114 desert environment by microclimate numerical simulation. Kong et al. [5] declared that trees  
115 planted in high density settings were more effective in improving pedestrians' thermal  
116 comfort than those in open spaces, and trees with a large crown, short trunk, and dense  
117 canopy were the most efficient in reducing mean radiant temperature. They recommended  
118 some specific ways to facilitate the integration of tree planting into urban design. For  
119 instance, trees with larger crowns are preferable and a closer spacing offers continuous  
120 shading in the street environment; parallel rows of trees should be used in wider streets.

121 Morakinyo et al. [22] developed the approach of sky-view factor mapping to aid tree  
122 selection for multiple ecosystem services of trees. They suggested that dense foliage trees  
123 of an average height, such as *Bauhinia blakeana* (~7 m, LAI 3.55), *Macaranga tanarius* (~4  
124 m, LAI 3.02), and *Aleurites moluccana* (~9 m, LAI 2.77), should be planted in high sky-view  
125 factor areas or locations e.g. shallow street canyons and other open spaces, while tall trees  
126 with sparse foliage should be planted in low sky-view factor areas such as deep canyons.  
127 The sky-view factor oriented planning approach was tested in Tan et al. [34] in designing  
128 outdoor comfort and climate resilience in subtropical high-density cities. Morakinyo and Lam  
129 [35] conducted a simulation study on the impact of tree-configuration, planting pattern and  
130 wind condition on street-canyon microclimate under hot-humid climate conditions.  
131 Additionally, Kjellgren and Montague [36] showed that trees grown over asphalt had up to  
132 6°C higher leaf surface temperatures than those over turf; it also demonstrated up to 3°C  
133 variation in leaf surface temperature between the species tested. Nevertheless, trees'  
134 thermal performance has not yet been taken into account, from the perspective of their  
135 physical characteristics, in the establishment of urban planting guidelines, mainly due to  
136 limited information or understanding.

137  
138 Scrutinising existing literature on urban trees reveals a lack of information on their radiative  
139 thermal performance, especially in the infrared (IR) region. This gap is an important one to  
140 address because IR radiation accounts for 52.4% of the terrestrial solar radiation reaching  
141 on the earth on south facing surface tilted 37° from horizontal [37]. Urban green spaces and  
142 trees are known to interact with solar IR radiation in a way that is dramatically different to  
143 the way they deal with visible (VIS) solar radiation via photosynthesis. Bridging the gap is  
144 thus crucial for fully understanding the role and potential of tree cooling effects. Previous  
145 studies on trees' radiative performance can be broken down into two main areas. The first  
146 area is studies that were mainly concerned with measuring individual leaves in the  
147 laboratory and field [38–42]. An interesting study in this area was done in the context of a  
148 different engineering discipline, aimed at cooling photovoltaic cells for maximising their  
149 electrical output in the light of tree leaves and tree bark spectroscopy [43]. The second is  
150 those studies that have focused on the radiative performance of tree canopies at a regional  
151 scale [44–46], which present a significantly different challenge to the tree leaf level. This is  
152 mainly because characterising the infrared radiative performance of trees at the tree crown  
153 level is complicated by the diverse morphologies and complex crown architecture of trees,  
154 as well as the temporal variation in solar radiation received throughout a day and over the

155 course of a year. Importantly, there is no easily applied standard characterisation method  
156 available to investigate the radiative performance of trees.

157

158 This paper presents a novel study on both leaf level and crown level interactions between  
159 lime trees (*Tilia cordata*) and solar radiation. The study was aimed at providing information  
160 on the variation between individual trees in IR radiative performance of both individual  
161 leaves and tree crown surfaces to lay a foundation for a better understanding of the cooling  
162 potential of tree species. The work entailed significant reassessment of previous  
163 methodologies and concepts, in order to establish appropriate techniques for characterising  
164 urban tree interaction with solar IR radiation. The new conceptual and methodological  
165 framework was then applied to study trees in urbanised settings, generating valuable  
166 insights into intraspecific variation in the radiative performance of lime trees at the leaf and  
167 crown levels.

168

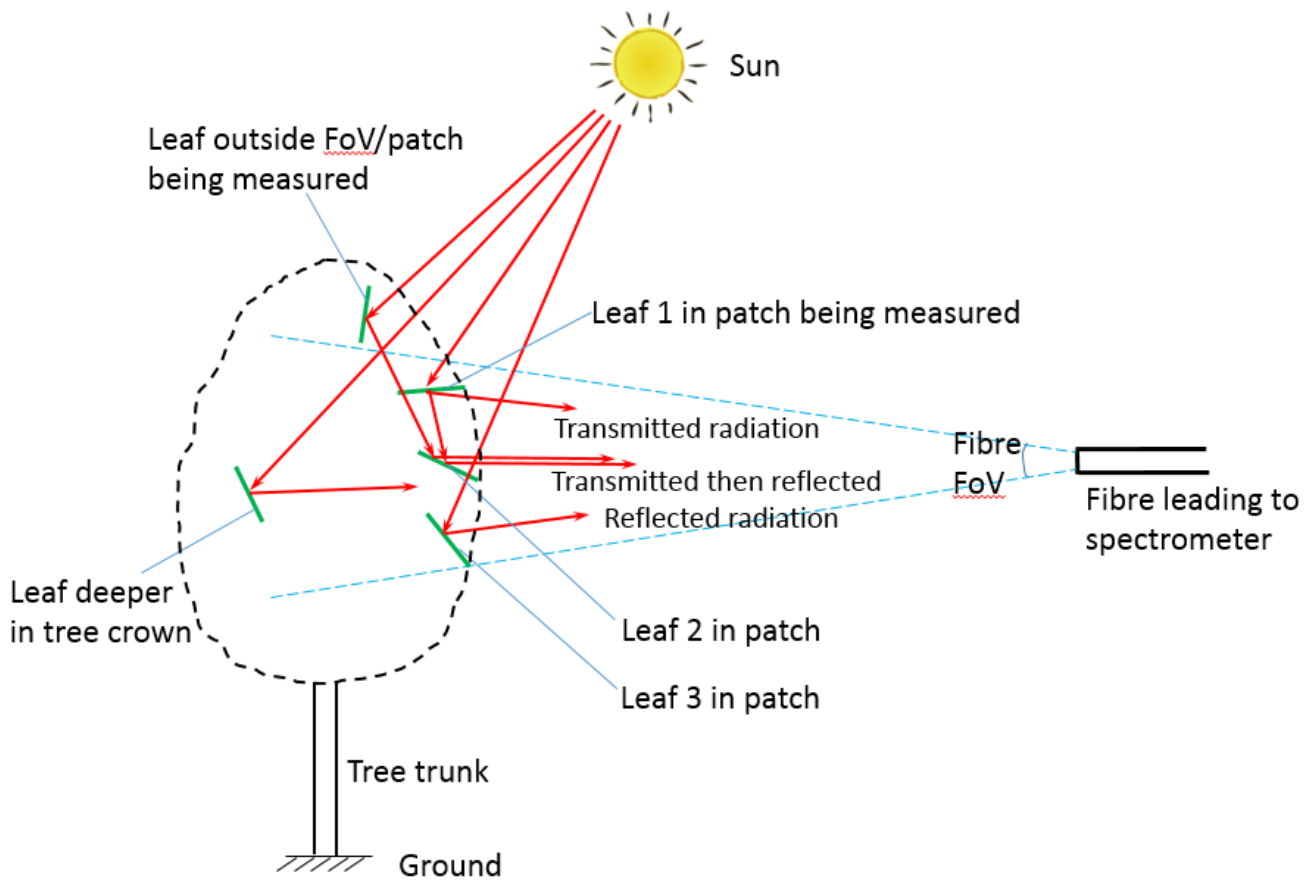
## 169 **2 Concepts for tree crown spectroscopy**

### 170 **2.1 Transflection and transfectance**

171 The radiative properties of individual tree leaves are characterised by absorbance,  
172 reflectance and transmittance of leaves, which can be measured separately. Yet, the  
173 radiative performance of the whole tree cannot be determined in terms of the radiative  
174 properties of tree leaves. The radiative performance of trees is rather complex compared to  
175 single leaves due to tree morphology, tree architecture and temporal variation of solar  
176 radiation. It is impractical to separate solar radiation transmitted through or reflected off  
177 various tree leaves, even if a fraction of the 'crown surface' is studied. Figure 1  
178 schematically illustrates the tree crown interaction with solar radiation. When an optical  
179 sensor (i.e. fibre spectrometer) is positioned at one side of the tree to measure the radiative  
180 performance of 'a patch of tree crown surfaces' (abbreviated as 'a patch' hereafter), the  
181 received light of the spectrometer might comprise single-reflected, multi-reflected, multi-  
182 transmitted and transmitted-reflected rays through leaves. In this sense, it is necessary to  
183 introduce the term, transfectance (transflection) to describe the integrated radiative  
184 performance of trees at the crown level. This is not to be confused with the technique of  
185 spectral measurement used in near-infrared spectroscopy.

186





187  
 188 Figure 1. Tree crown-level interactions with solar radiation, illustrating the concepts of  
 189 transfectance (transflection) for a patch being measured; FOV=Field of View

190  
 191 To establish the measurement method of the transfectance of tree crowns, it is useful to  
 192 first scrutinise the definitions of radiative properties of individual leaves and then devise  
 193 methods. At the leaf level, leaf reflectance is measured by the ratio of the reflected radiation  
 194 from a given leaf to the reflected radiation from a reference plane with a reflectance  
 195 standard that replaces the leaf at the same position, as shown in Equation (1). Both of the  
 196 reflected types of radiation are measured by a spectrometer. Similarly, a leaf-level  
 197 transmittance is obtained by the transmitted radiations from a given leaf and the reflectance  
 198 standard that replaces the position of the leaf, as given by Equation (2).

199  
 200 
$$r = \frac{I_{reflected}}{I_{ref}} \quad (1)$$

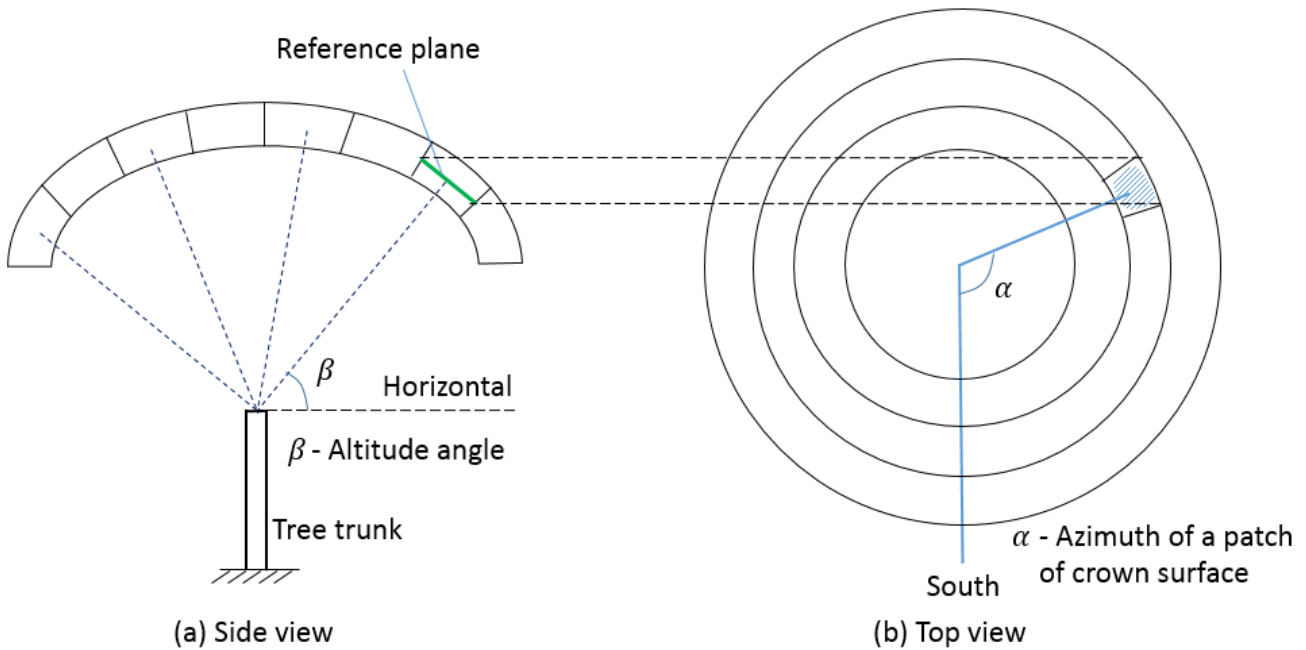
201  
 202 where  $r$  is reflectance,  $I_{reflected}$  is the reflected radiation from a given leaf and  $I_{ref}$  is the  
 203 reflected radiation from a reference plane with a reflectance standard.

204  
 205 
$$\tau = \frac{I_{transmitted}}{I_{ref}} \quad (2)$$

206  
 207 where  $\tau$  is transmittance,  $I_{transmitted}$  is the transmitted radiation from a given leaf.

208

209 For the tree crown level, the term transfectance of a patch of the crown surface should be  
 210 used to define the ratio of the total reflected and transmitted radiation from the patch (and  
 211 received by the spectrometer fibre) to the reflected radiation from a reference plane with a  
 212 reflectance standard that replaces the patch. For each patch of the crown surface, the  
 213 reference plane for transfectance spectra measurement is the average plane of this patch  
 214 of the crown surface as indicated in Figure 2. Definition of the average plane is not quite  
 215 specific here, which is deliberate, because this concept will evolve further (see section 2.4).  
 216



217 (a) Side view  
 218 (b) Top view  
 219 Figure 2. An illustration of a tree model (model 1) showing azimuth and altitude angles and  
 220 reference plane location for a specific patch of crown surface

220

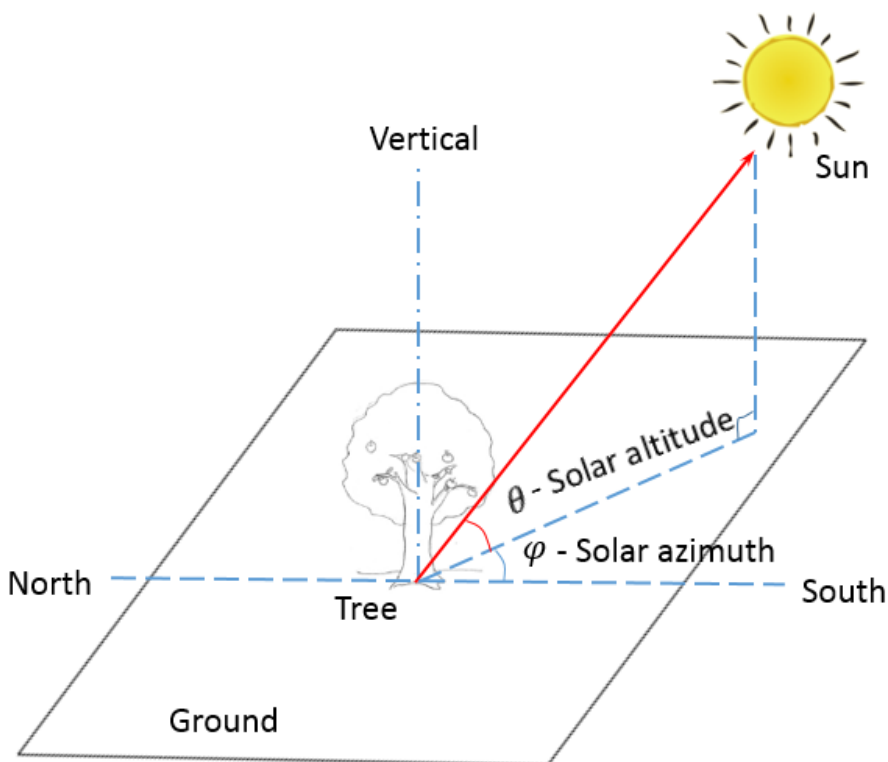
## 221 2.2 Six angles for characterising tree interaction with solar radiation

222 Figure 2 illustrates a tree model similar to an umbrella. Each small patch of crown surface  
 223 locations can be described by the two angles, azimuth ( $\alpha$ ) and altitude ( $\beta$ ). To fully  
 224 characterise the tree interaction with solar radiation, two more pairs of angles are required.  
 225 One pair of angles is azimuth and altitude of the sun, shown in Figure 3, allowing a  
 226 description of the effect of different solar positions, seasons and time of day. Another pair of  
 227 angles is azimuth and altitude of the viewing direction of the spectrometer optical fibre in  
 228 relation to the patch of crown surface, shown in Figure 4, which helps to characterise the 3-  
 229 dimensional variation of the transflected solar radiation from the tree crown surfaces. Thus,  
 230 in total, 6 angles (Figures 2–4) are needed to map a tree’s interaction with solar radiation.  
 231 Even if each angle is discretised into 10 values in space, which is still rather coarse to  
 232 characterise the whole tree crown, a total of one million transfectance spectra would need

233 to be obtained. When finer resolutions are required, even greater numbers of spectra would  
234 be needed, which would be impractical to achieve. In this sense, rather than a full mapping  
235 for each tree, a first step would be to identify a small number of important factors affecting  
236 the tree-solar radiation interactions and focus on understanding the nature and magnitude  
237 of their effects.

238

239 Urban tree research often deals with the effect of trees on buildings and people. In this  
240 context, the spectra of solar radiation received by a building or a person can be obtained  
241 through the integration of those from each of the small patches with different angles to the  
242 building or the person.

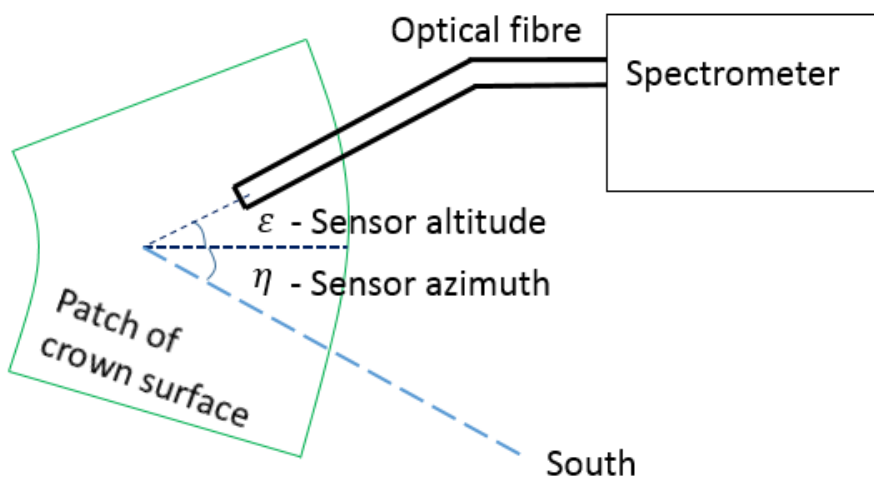


243

244 Figure 3. An illustration of solar azimuth and altitude angles in relation to a tree being

245

studied



246

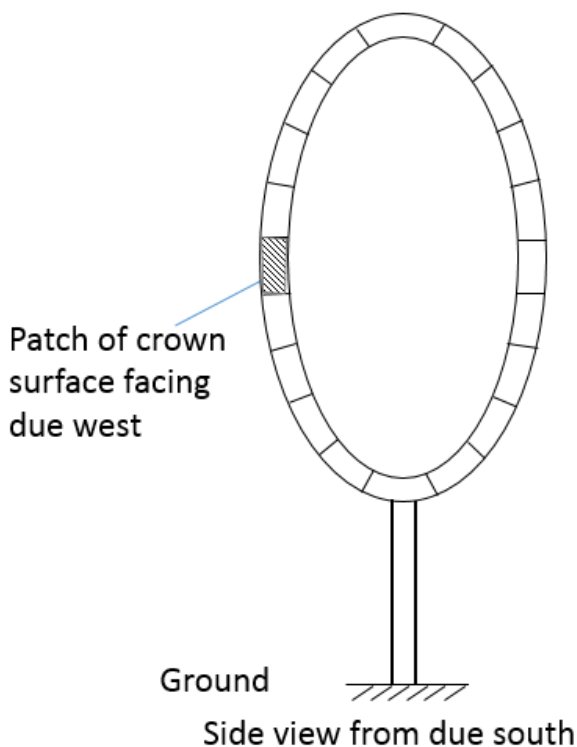
247 Figure 4. An illustration of a patch of crown surface showing azimuth and altitude angles for  
248 the spectrometer optical fibre

249

### 250 2.3 Reference plane and contributing volume

251 In a leaf-level measurement scenario, the light falling on the leaf is all that is available for  
252 reflection off or transmission through the leaf. In contrast, in the situation of crown-level  
253 measurement, for any patch of crown surface being measured, light falling on other parts of  
254 crown beyond the measured patch of crown surface can contribute to the transflected solar  
255 radiation received by the spectrometer /fibre directed on this patch. As shown in Figure 1,  
256 solar radiation transflected by foliage located deeper into the crown beyond the patch of  
257 crown surface, and by foliage located outside the field of view (FoV) of the spectrometer  
258 optical fibre, can contribute to the measured solar radiation spectra. Namely, light from a  
259 volume of the crown rather than from just the reference surface for the patch being tested is  
260 influencing the spectra measurements, as illustrated in Figure 5, which presents a common  
261 tree crown form. Thus at the crown level, the concept of contributing volume, in conjunction  
262 with the reference plane, is important for understanding and interpreting transreflectance  
263 results.

264



265

266

267 Figure 5. An illustration of tree model 2 and contributing volume

268

269 **2.4. Single versus multiple reference planes**

270 In the tree model 1 discussed, the concept of a reference plane for each patch of the crown  
271 surface is introduced (Figure 2). However, there is a degree of arbitrariness to the selection  
272 of this reference plane position. This is due to the variation of leaf surface orientation,  
273 density, position, etc. Furthermore, the reference planes for different patches of the crown  
274 surfaces have diverse orientations so their reference spectra are different, making  
275 comparisons of solar IR performance among different patches (e.g. those facing four  
276 cardinal directions revolving around E, S, W, N) of the crown surface rather difficult. Finally,  
277 more importantly for the tree model 2 presented in Figure 5, the method of selecting the  
278 reference planes for each patch will break down in some cases. For example, at midday, a  
279 patch of crown surface facing north has a reference plane which receives no direct sunlight,  
280 while the contributing volumes beyond this patch ensure that the patch will still project  
281 outwards a significant amount of solar radiation. The resulting spectra will have infinite  
282 values throughout the wavelength range of the spectrometer, thus a measurement might  
283 not be useful at all. Likewise, patches of the crown surface in the shadow sides of the tree  
284 will experience a similar problem.

285

286 It was therefore decided that for a single tree, the measured spectra for various patches of  
287 the tree crown surface would be referenced to a single (or fixed) reference plane. It is our  
288 recommendation that a flat surface vertical to the horizontal ground facing directly to the  
289 sun (i.e. perpendicular to the projection of the sunlight line to the horizontal ground) should  
290 be chosen. There is no rigid principle of choosing the single reference plane, but once  
291 selected the single reference plane will allow quantitative comparisons of different patches  
292 of the tree crown surfaces. Note that in principle, surfaces of any orientation could be  
293 chosen. Furthermore, the measured spectra on a specified reference plane can be  
294 transformed to corresponding spectra in relation to a different reference plane with a  
295 different orientation. A vertical reference plane is chosen in this study because it is more  
296 intuitive and urban built surfaces are often vertical. More significantly, at a practical level,  
297 during early morning or late afternoon a vertical reference plane would avoid the situation  
298 where the sunlight is at a shallow angle to the reference plane, resulting in reference  
299 spectra being sensitively affected by minute deviation from the horizontal by the reference  
300 plane.

301

302 **3 Test setup**

303 **3.1 Test site and studied trees**

304 One common urban tree species, *Tilia cordata* (or small-leaved lime) was chosen to measure  
305 the radiative energy exchange of the trees during August and September, 2018. The test  
306 programme included a total of 10 *Tilia cordata* (numbered as 'Tilia 1–10') growing in a plaza  
307 surrounded by four-storey modern Halls of Residences on the campus of the University of  
308 Reading, Berkshire, UK, as shown in Figure 6. The height of the *Tilia* trees was between 5.4-  
309 6.0 m with a crown height of 1.6–2.0 m and crown diameter of 3.0–3.6 m. *Tilia* 1 was tested  
310 more often than the other *Tilia* trees given its convenient location in the test site (see Figure  
311 6 (b)). *Tilia* 7, 8 ,9 formed a cluster. *Tilia* 7 tended to be the visually most healthy (greener,  
312 more foliage) tree and *Tilia* 10, the visually least healthy tree in the group.

313



(a)



(b)



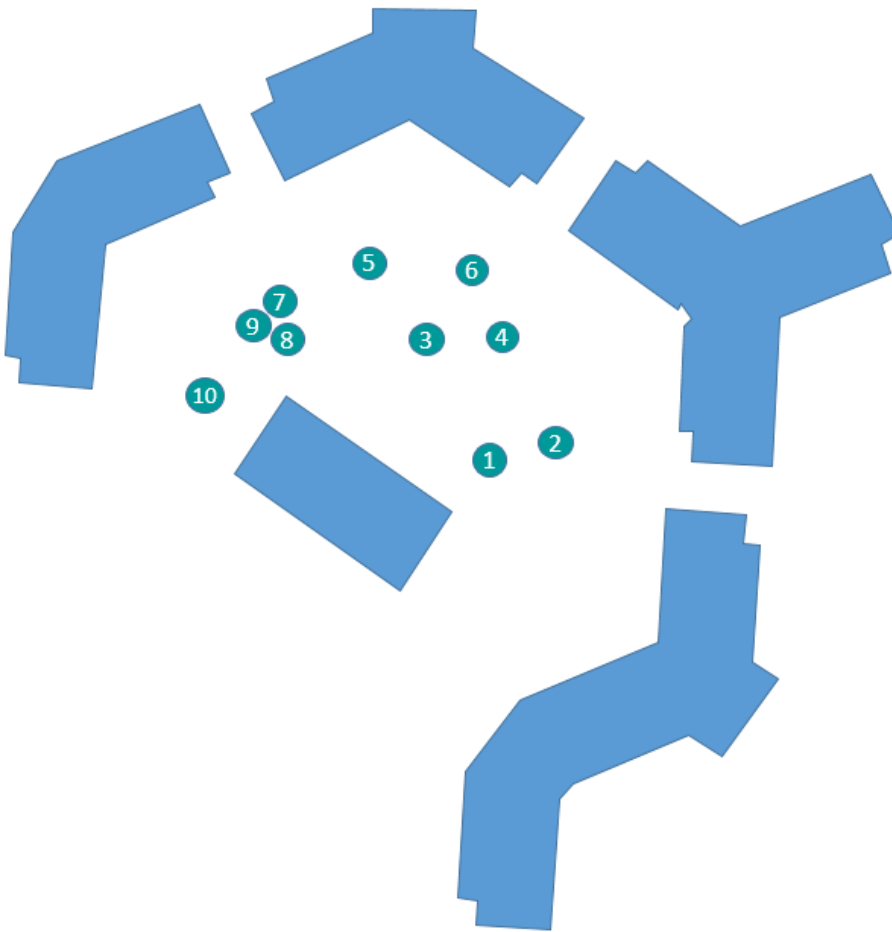
(c)



(d)

314

315 Figure 6. Test site and *Tilia* trees (a) 3-9, (b) 1 and a tripod holding a spectrometer, sampling  
316 fibre and laptop, (c) 1 in foreground, 2 to the right, (d) 7-9 (right to left)



317  
318 Figure 7. Schematic showing location of the 10 *Tilia cordata* trees

319

### 320 3.2 Test instruments

321 Measurements of reflection and transmission spectra of individual tree leaves and  
322 transflection of tree crowns were carried out in the visible (VIS) and near infrared (NIR) ranges,  
323 using a combination of VIS and NIR spectral analysers up to 2500 nm wavelength.

324

325 A Spectral Evolution spectrometer (model SM2500, made in USA) with spectral resolution of  
326 3.5–22 nm in the full range of UV (ultraviolet), VIS, NIR (wavelength range: 350–2500 nm  
327 and wavelength reproducibility of 0.1 nm at an accuracy of 0.5 bandwidth) was used mainly  
328 in the laboratory to measure leaf level reflection and transmission of solar radiation within the  
329 range of 350-2500 nm. This was the spectrometer with the broadest spectral range. It was  
330 also the most bulky one and not suitable for mounting on a tripod for field canopy  
331 measurements.

332

333 A StellarNET Black-Comet concave grating miniature spectrometer (model CXR, made in  
334 USA) with a wavelength range of 350-900 nm and a spectra resolution of 0.5 nm was used  
335 for field canopy tests. This covers the full VIS spectrum of 400-700 nm. It also covers the  
336 important spectrum transition from VIS to NIR around 700 nm where the leaf and crown  
337 transmission and reflection jump sharply as shown in all measured spectra presented in the  
338 following. The spectra also show the peak of reflection or transmission in the IR region, which  
339 occur usually immediately following the VIS-IR transition. As can be seen in the reflectance  
340 spectra obtained using the Spectral Evolution SM2500 (see Figure 9 in section 4.2) or other  
341 published tree leaf spectra to 2500 nm [31–34], the reflectance and transmittance drop  
342 monotonically and predictably to levels close to 0 around 2500 nm if two water absorption  
343 troughs around 1400 nm and 1900 nm are excluded. Given this largely predictable pattern  
344 beyond 900 nm, much information about the NIR behaviour of trees can be obtained by using  
345 the miniature spectrometer, which is much lighter and smaller, for field work. It is also much  
346 cheaper and can be more quickly replaced as required.

347  
348 A third spectrometer, a StellarNET Black-Comet-SR concave grating miniature spectrometer  
349 (model CXR-SR), has a spectroradiometer mode which allows the irradiance of the radiative  
350 energy received by the optical fibre fitted with a cosine receptor of 180° field of view to be  
351 displayed for every 0.5 nm wavelength intervals in the 400-1100 nm range (350-1030 nm  
352 with acceptable signal-to-noise ratio). It was used for solar irradiance spectra measurements  
353 as it was specifically calibrated for such tests.

354

### 355 **3.3 Test procedures**

356 A tripod with a full height of 4 m was used to hold and position the optical fibres of  
357 spectrometers in the field tests. An optical fibre was mounted onto the top of the tripod at  
358 one end and connected to a StellarNET Black Comet miniature spectrometer at the other.  
359 The portable spectrometer had a spectral range of 350-900 nm and was powered through  
360 an USB cable connected to the data acquisition laptop. The same USB cable also served  
361 as the data transmission between the spectrometer and the computer. The battery fully  
362 charged usually lasted for about five hours powering both the laptop and the spectrometer.  
363 Viewing angle of the optical sensor can be adjusted in all directions. The optical fibre was  
364 usually used without any cosine receptor and had a field of view of 25°.

365

366 Different scenarios were devised to identify important influence factors on tree's radiative  
367 performances. To begin with, reflected and transmitted radiative energy from individual



368 leaves was measured to quantitatively ascertain the predominant radiative energy of trees  
369 in the IR region. Then the reflectance spectra of individual leaves from different lime trees  
370 were measured to provide a contrast with the transfectance spectra at the tree crown  
371 levels. Measurements of various viewing angles of the optical sensor (fibre spectrometer)  
372 and different directions around the crown, representing different azimuth angles of the  
373 optical sensor, were performed on a single tree (*Tilia* 1) to distinguish the differences. The  
374 transfectance spectra among all 10 lime trees were also explored. To better understand  
375 trees' radiative performance at the crown levels, on-site measurements of transmission and  
376 reflection spectra of leaves with different fibre viewing angles and different leaf orientations  
377 were implemented to supplement the interpretation. The reference plane for the crown  
378 transfectance spectra measurements was chosen in a vertical plane towards the sunlight  
379 direction. Some other testing details are described alongside the results in the following  
380 section.

381

382 As to the test conditions, all the tests were performed under cloudless blue sky conditions.  
383 This is mainly because a sky with even patchy or thin clouds could result in significantly  
384 different solar radiation conditions within a few seconds. Clouds composed of water  
385 droplets will dramatically affect the IR solar radiation intensity reaching the trees due to  
386 water's characteristic strong solar absorption at specific IR wavelengths. It is hard to obtain  
387 the transfectance under such changeable solar radiation conditions, as the translected  
388 radiations of a specified patch and those of the corresponding reference plane would  
389 probably not be obtained under the same solar radiation conditions even when they are  
390 measured within several minutes. Furthermore, prior planning is needed and a set of tests  
391 is completed in quick succession, typically within a few minutes, so that the sunlight  
392 conditions remain virtually unchanged, making the comparisons among the set of test  
393 results feasible. For this study, weather data were recorded at the University of Reading  
394 Meteorology Observatory 100 m away from the test site.

395

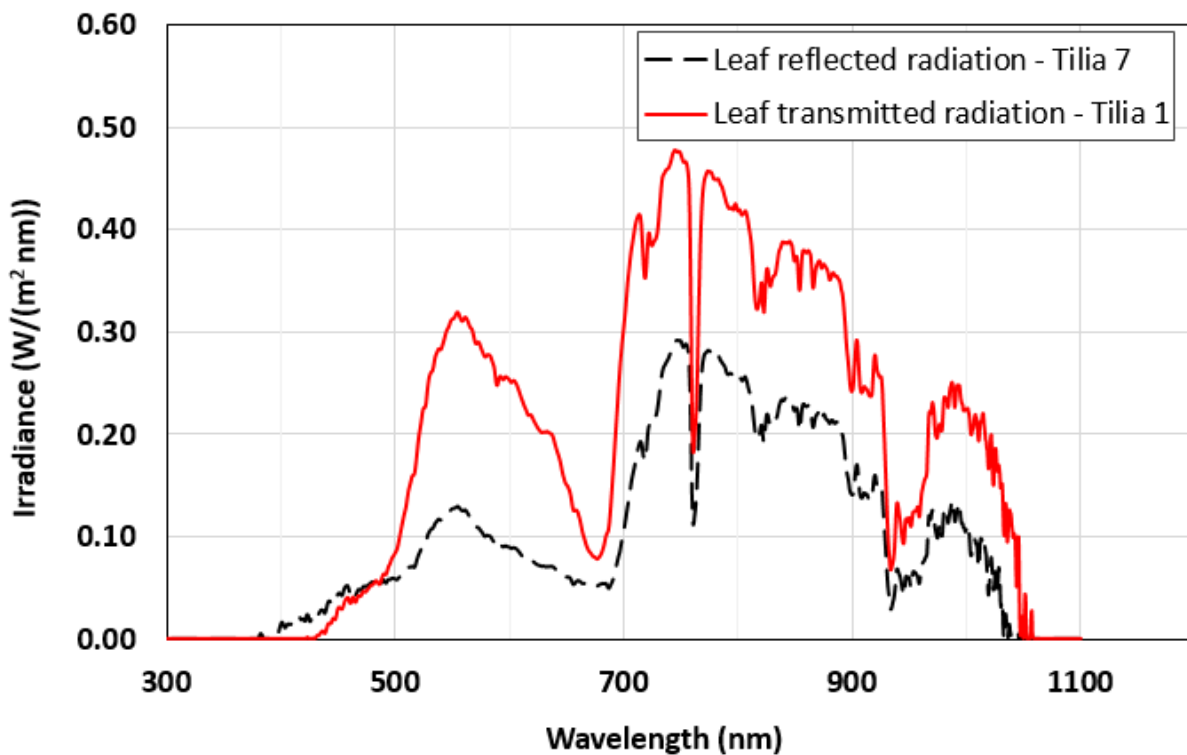
## 396 **4 Results and discussion**

### 397 **4.1. Reflected and transmitted radiative energy spectra of leaves**

398 An example for an irradiance spectrum of the light reflected from a leaf on *Tilia* 7 (see  
399 Figure 6 (d)) is given in Figure 8. The miniature spectrometer with a spectroradiometer  
400 mode was used to measure the irradiance. The measurement was made during a period  
401 with clear cloudless sky between 1–2 pm BST on 27<sup>th</sup> September 2018 (Outdoor dry/wet  
402 bulb temperatures 20.6–21.1 °C / 13.8–13.9 °C; relative humidity 42–44%; horizontal global

403 solar irradiance 503.2–580.7 W/m<sup>2</sup>; horizontal diffuse radiation 52.7–54.4 W/m<sup>2</sup>; wind  
404 speed 2.8–2.9 m/s). The leaf was fully illuminated by sunlight and reflected light was  
405 sampled in a direction vertical to the leaf surface. Although the spectrum was not extended  
406 to 2500 nm as in spectra obtained using the Spectral Evolution SM2500 Spectrometer, it  
407 was clear from Figure 8 that the reflected energy was dominated by the IR radiation, which  
408 accounted for 74.0% of the whole reflected energy measured, assuming 700 nm as the  
409 demarcation line of VIS and IR regions. Figure 8 also provides an example of an irradiance  
410 spectrum of light transmitted through a leaf on *Tilia* 1 (see Figure 6 (b) or (c)). Likewise, the  
411 transmitted radiative energy was dominated by the IR radiation with a high percentage of  
412 70.1%. It can be seen that proportionally, the VIS part of the irradiance spectrum for *Tilia* 1  
413 is larger than that for *Tilia* 7. This larger VIS irradiance was also observed in the reflection  
414 spectrum for *Tilia* 1 and was in line with the visual observation that *Tilia* 1 was more  
415 stressed than *Tilia* 7 (greater yellowing of leaves).

416



417

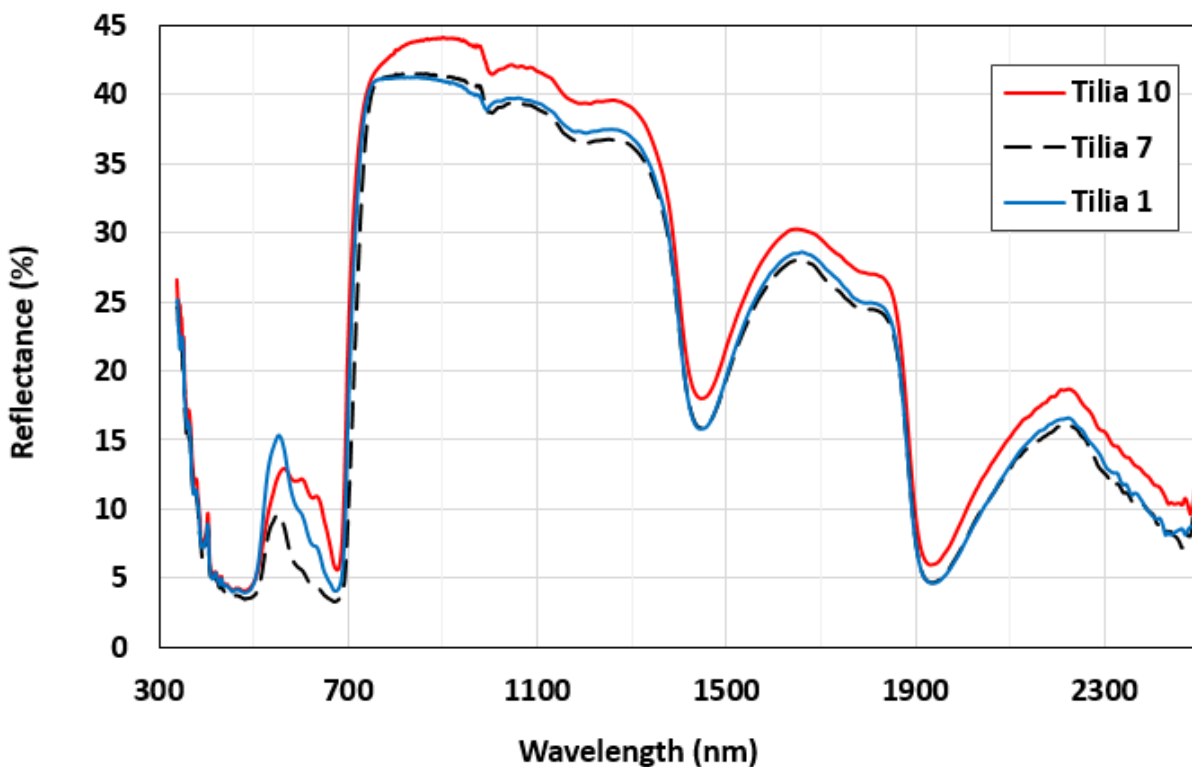
418 Figure 8. Samples of the reflected irradiance spectrum from a leaf on *Tilia* 7 and the  
419 transmitted irradiance spectrum from a leaf on *Tilia* 1

420

421 **4.2. Reflectance spectra of individual leaves in the laboratory**

422 The individual leaves from all 10 *Tilia* trees were collected then immediately scanned on  
423 11<sup>th</sup> September 2018 to generate the reflectance spectra of the leaves in the laboratory  
424 using the Spectral Evolution SM2500 spectrometer. The spectrometer was deployed  
425 together with a leaf clamp, which was purposely built and supplied by the spectrometer  
426 manufacturer for measurement of reflectance spectra of leaves. Measurements using the  
427 clamp resulted in spectra data which were very repeatable, i.e. multiple scans of leaves in  
428 the clamp produced nearly identical spectra.

429 The leaf reflectance spectra of *Tilia* 1, *Tilia* 7 and *Tilia* 10 (see Figures 6 and 7 for the  
430 location and images of the trees) have been given in Figure 9. *Tilia* 7 tended to be the  
431 visually most healthy (greener, more foliage) tree and *Tilia* 10, the visually least healthy tree  
432 in the group. As seen in Figure 9, the leaf level spectra were broadly similar, despite  
433 significantly different (stress) conditions of the trees /leaves. The spectra differences  
434 between individual leaves are less than 5% in the IR region. Their similarity at the leaf level  
435 is in contrast to the significantly greater differences among crown transreflectance spectra of  
436 the corresponding trees discussed in the following sections.



437  
438 Figure 9. Leaf reflectance spectra of *Tilia* 10, *Tilia* 7 and *Tilia* 1 in question

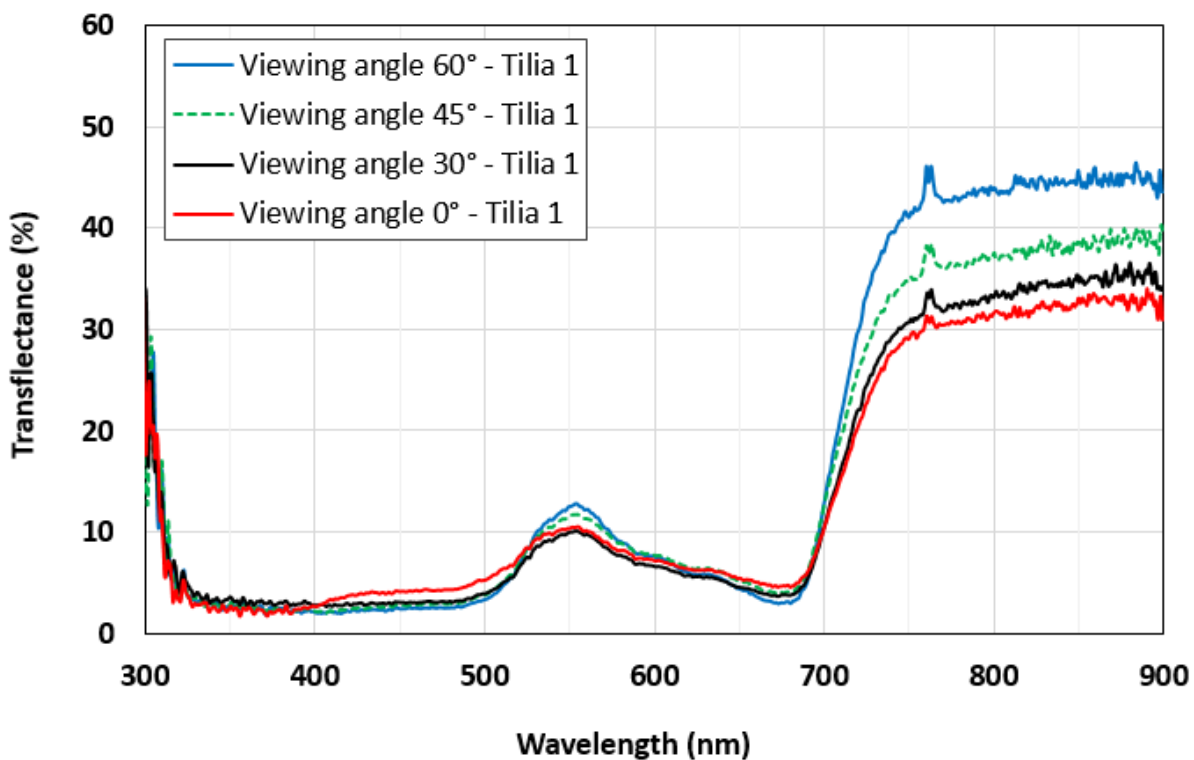
439

440 Also worth noting is the broader VIS reflectance spectrum distribution of the leaf for *Tilia* 10  
441 which was more affected by the summer drought and showing greater yellow/brown  
442 colouring in the leaves. This is a repeated feature of drought stress leaves that are  
443 yellower/browner.

444

#### 445 **4.3. Transflectance spectra of single tree crown – effects of viewing angles**

446 The transflectance spectra presented in Figure 10 were measured between 9:45-10:45 am  
447 on 1<sup>st</sup> September 2018 in a clear sky. The transflectance spectra at the viewing angles 0°,  
448 30°, 45° and 60° of the optical fibre were measured - Fibre tip at the top of the tripod setup  
449 pointed initially horizontally towards the crown at a distance of about 2.5 m from the tree  
450 trunk centre. The fibre tip was then tilted to form an angle of 30° to the horizontal plane  
451 looking downwards. This angle was then increased progressively to 60°. The fibre was set  
452 in a plane vertical to the ground and parallel to the solar azimuth direction.

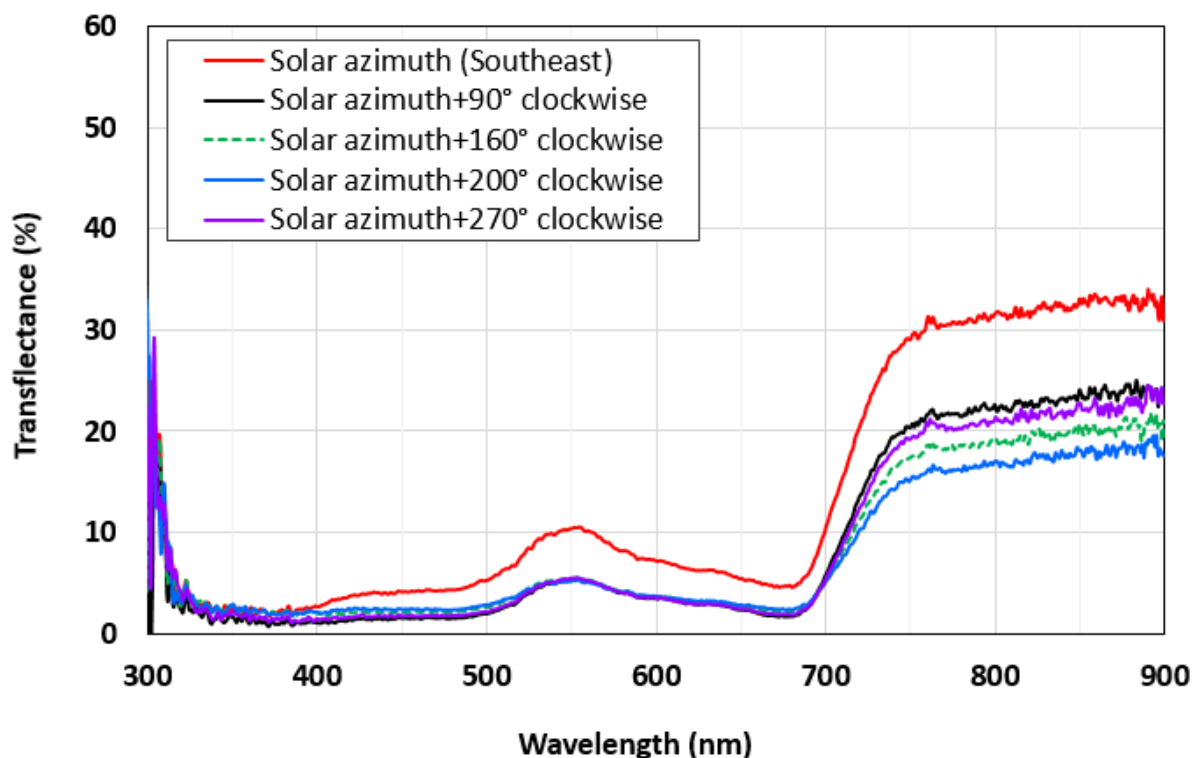


453 Figure 10. *Tilia* 1 transflectance measurement – effect of viewing angles of the optical fibre  
454 in a vertical plane  
455

456  
457 Figure 10 shows that the transflectance measured on *Tilia* 1 increases with the fibre viewing  
458 angle from 0° (horizontal) through to 60° (looking downwards). This monotonic increase  
459 with measurement angles is not always so in all tests (due to local foliage characters /non-  
460 uniformity of the crown structure in terms of leaf density, number and angular distributions,

461 etc). However, among the tests carried out, the highest IR transfectance were generally  
462 found at an angle deviating from the horizontal plane rather than in the horizontal directions.  
463

464 Figure 11 shows of the transfectance spectra measured from four cardinal directions  
465 around the tree crown. All spectra presented were obtained with the horizontal viewing  
466 angle ( $0^\circ$ ) of the optical fibre. The tests were performed in the morning during 9:45–10:45  
467 am BST. Crown transfectance measured horizontally in the sunlight direction (Solar  
468 azimuth - southeast) was highest, that measured horizontally in the opposite direction (solar  
469 azimuth+ $200^\circ$  clockwise) was lowest, while the spectra measured in the two directions  
470 perpendicular to Southeast–Northwest, i.e. solar azimuth+ $90^\circ$  clockwise and solar  
471 azimuth+ $270^\circ$  clockwise, fell in between. This ranking of transfectance levels measured in  
472 four directions around a tree is frequently observed in our tests and referred to as a ‘Classic  
473 Distribution’. Note that two directions of Northwest  $\pm 20^\circ$  were used rather than Northwest,  
474 ensuring that the optical fibre tip would not include the sun within its field of view.

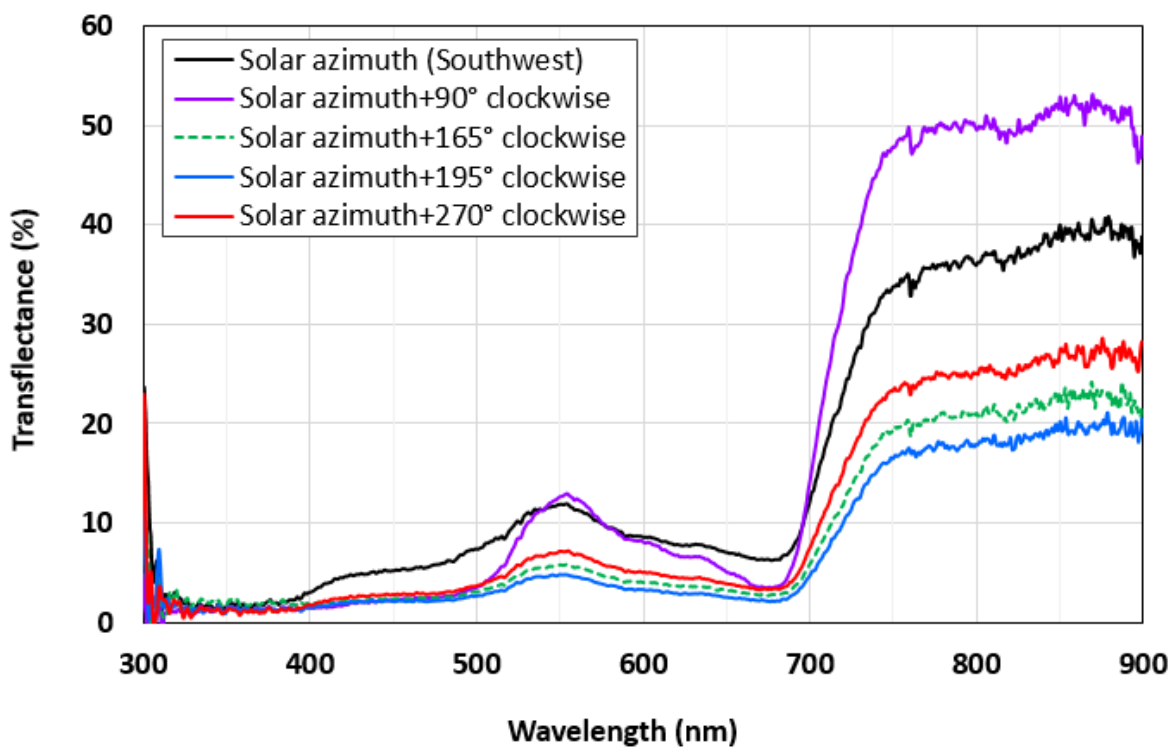


475  
476  
477 Figure 11. *Tilia* 1 transfectance measurement – spectra measured in four cardinal  
478 directions around the tree during 9:45–10:45 am BST

479  
480 In contrast to the transfectance tests of four cardinal direction distributions in the morning,  
481 the results obtained at 2 pm in the afternoon were more spread out vertically, with the

482 transfectance ranging from 20% to 50% as displayed in Figure 12. The significant  
 483 differences between Figures 11 and 12 indicate that tree canopy transfection distribution is  
 484 not only a property of the tree crown but also varies with solar time. Moreover, the  
 485 distributions in Figure 12 also reveal a relatively less common situation where the highest  
 486 transfection levels were not found in the sunlight direction (Southwest) but at a direction  
 487 with 90° clockwise + sunlight direction (e.g. the highest transfection appeared in the  
 488 Northwest when the sunlight was in the Southwest direction). Visual observation showed  
 489 that the FoV of the spectrometer positioned at 90° + sunlight direction included some high  
 490 density and bright (suitably aligned with sun direction) leaf clusters. Such local characters or  
 491 non-uniformity of the tree crown is one of the key features of the crown architecture which  
 492 was found to affect significantly the tree crown / solar IR interactions. Our initial tests on  
 493 other species, e.g. oak, showed that the choice of tree species also had a substantial effect  
 494 on the four-direction transfection distributions, apparently due to crown structure  
 495 differences as well.

496



497

498

499 Figure 12. *Tilia* 1 transfectance measurement – spectra measured in four directions around  
 500 the tree at 2 pm BST

501

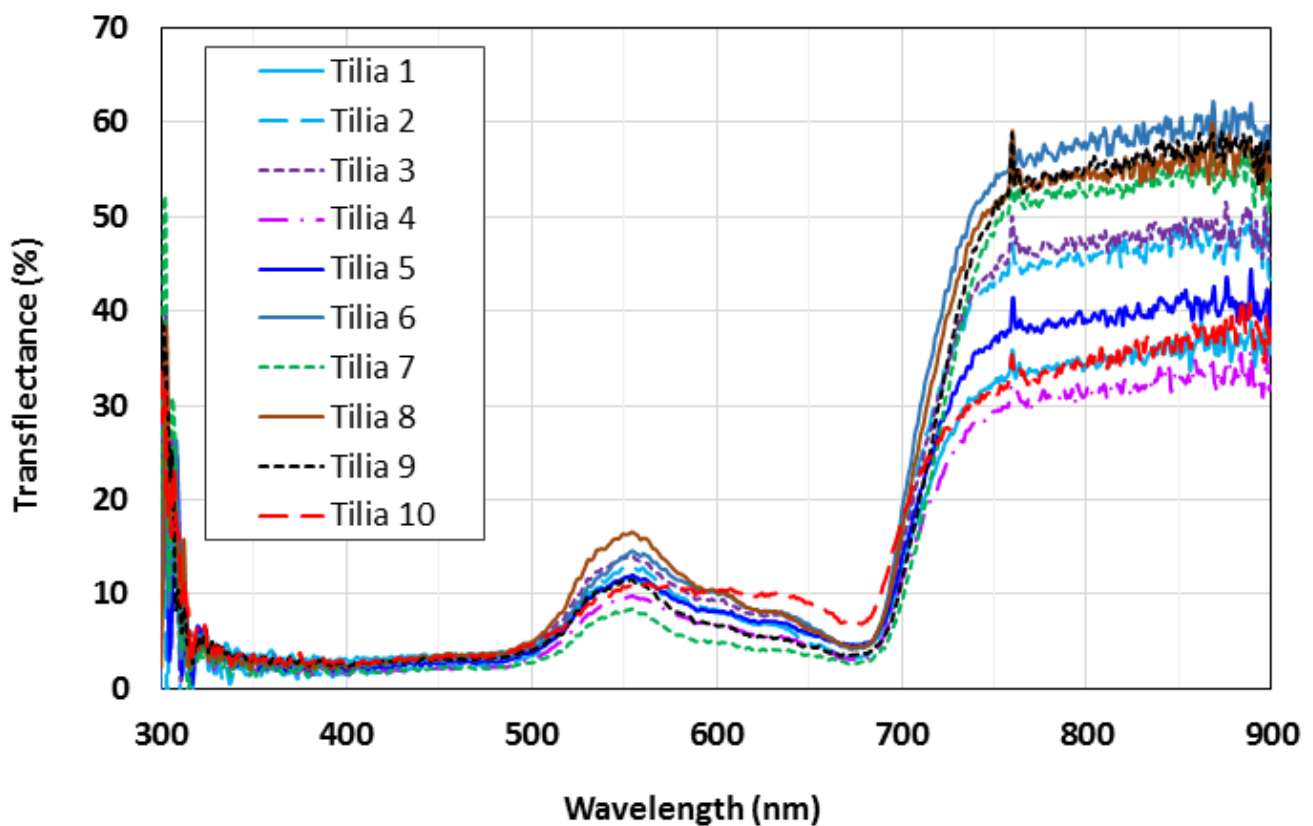
502 The variations among the transfectance spectra measured in the four cardinal directions  
 503 reveal that locational relationship of buildings and people to trees could sensitively affect  
 504 the levels of solar IR radiation they receive. Furthermore, the significant changes of

505 transfectance distributions with time show that buildings and people around a tree would  
506 not only receive different levels of solar IR radiation at different time, but the relative  
507 intensity of the solar IR radiation they receive will also change. As will be discussed further  
508 in the following, a significant factor for the change with time is the change of solar angle.  
509 Also important are changes of tree leaf angle and density in response to environment  
510 stress, although their effects will take longer to manifest and will also last over a relatively  
511 longer time-scale.

512

#### 513 4.4. Variation of IR radiative performance among trees in a single species

514



515

516 Figure 13. Transflectance spectra of all 10 *Tilia* trees

517

518 Figure 13 displays transflectance spectra of all 10 *Tilia* trees included in the study. These  
519 were measured during the period of 10:15–11:15 am BST on 6<sup>th</sup> September 2018 with a  
520 clear blue sky. For each of the 10 trees, the spectra were measured with the sampling  
521 optical fibre pointing in the sunlight direction horizontally and 30° downwards in a vertical  
522 plane.

523 *Tilia* 6, 7, 8, 9 exhibited the highest IR transfectance and the latter three formed a cluster.  
524 They generally had denser foliage among the tested trees. The clustered trees sheltered  
525 and shaded each other so that they were less thermally stressed. *Tilia* 7 was the most  
526 sheltered and had the lowest VIS peak in the cluster, while *Tilia* 8 being the least sheltered  
527 showed the highest VIS peak among the cluster of 3 trees. These were in line with the  
528 visual observation that *Tilia* 7 was greener (greater/healthier chlorophyll content in foliage)  
529 and *Tilia* 8 was slightly more affected by the hot dry summer with more yellowish patches.

530 *Tilia* 1, 4, 5, 10 exhibited the lowest IR transfectance spectra among the 10 tested trees.  
531 *Tilia* 10 was the most seriously affected by the summer drought and heat stress and was  
532 visibly damaged. *Tilia* 1, 4, 5 were visibly greener and healthier but they shared with *Tilia* 10  
533 a common feature, i.e., relatively but visibly lower foliage density. *Tilia* 10 had grown larger  
534 than *Tilia* 1, 4, 5 prior to the drought year of 2018. The lower crown leaf density of *Tilia* 10  
535 probably resulted from leaf shedding during the drought. *Tilia* 10 also showed broader and  
536 higher VIS peak which was in line with the more brownish appearance of its drought  
537 stressed leaves.

538 The above results and discussions, together with the individual leaf spectra scan carried out  
539 in the laboratory using leaves from these 10 trees (Figure 9), indicate that the substantial  
540 variations among transfectance spectra of tree crowns are much more affected by the  
541 structure of the crown (e.g. leaf number, density, etc) than by the character of the leaves  
542 (yellower, greener, more or less stress by drought etc).

543 The same contrasting results also highlighted the fact that despite similarity among  
544 reflectance and transmittance spectra at leaf levels, crown level spectra of the trees tested  
545 exhibit significant differences, thus confirming the importance of carrying out crown level  
546 investigations.

547

#### 548 **4.5. On-site measurement of leaf transmission and reflection spectra - effect of** 549 **viewing angles**

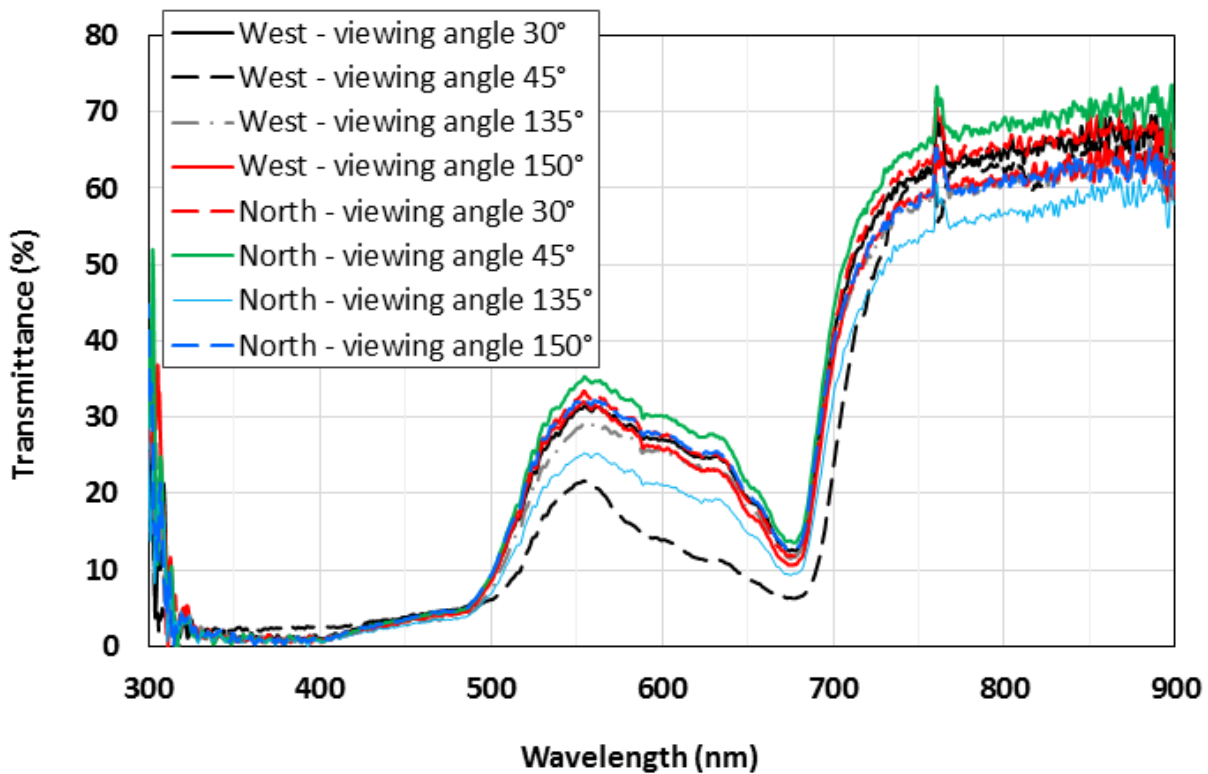
550 Figure 14 shows spectra of light transmission through a single leaf on *Tilia* 1. It was close to  
551 the bottom of the canopy thus could be easily reached by the spectrometer optical fibre.  
552 The leaf was fully sunlit and visually in average condition with slight signs of drought stress  
553 (yellowing). The leaf orientation was largely horizontal with a slight slope towards  
554 Southeast. The tests were carried out during the period of 10:15–11:15 am BST on 6<sup>th</sup>  
555 September 2018 with a clear blue sky. The transmission spectra were measured with the



556 sampling optical fibre pointing towards the centre of the back of the leaf, forming various  
557 viewing angles to the leaf surface (30°–150°) within two measured planes that were  
558 perpendicular to each other (W & N) and were both perpendicular to the leaf surface.

559 A single reference plane was adopted to allow the direct comparison of transmitted and  
560 reflected solar radiation measured at various viewing angles. This single reference concept  
561 is adopted here for leaves, also because the resulting spectra will later be used to offer  
562 insightful explanations of crown level spectra results. The reference plane azimuth was the  
563 same as that of the sun and the plane was perpendicular to the ground. This is the reason  
564 that some of the spectra contain values greater than 70%.

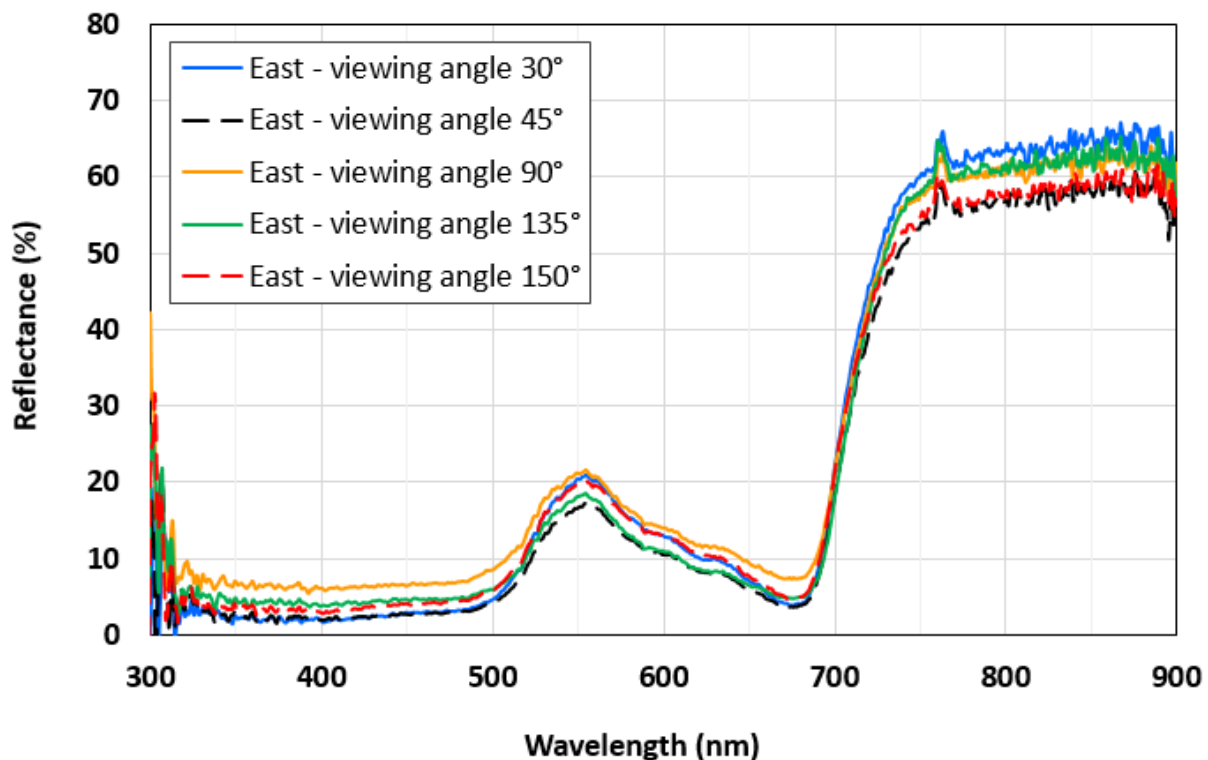
565 Figure 14 shows that the spectra are relatively close to each other despite the vast variation  
566 of the transmission directions.



567

568 Figure 14. Leaf transmission spectra measured from various viewing angles

569



570

571 Figure 15. Leaf reflection spectra measured from various viewing angles

572

573 Figure 15 similarly shows spectra of light reflection from a single leaf in *Tilia* 9. The leaf  
 574 location orientation and conditions were very similar to those for the transmission  
 575 measurements shown in Figure 14. Also similar were the test time and sampling optical  
 576 fibre arrangement except that in this case, the fibre pointed towards the centre of the top of  
 577 the leaf. The reflection spectra were obtained in one of the planes vertical to the leaf. As  
 578 seen in Figure 15, all spectra were again close to each other despite the large variation of  
 579 the reflection directions.

580 The spectra in Figures 14 and 15 show a modest effect of the viewing angle which resulted  
 581 in differences of about 10% among the spectra in the IR region. They are in contrast to the  
 582 diverging spectra seen Figures 16 and 17 presented in the next section, where the dramatic  
 583 effect of the leaf angle on reflected and transmitted IR and VIS radiation was revealed.

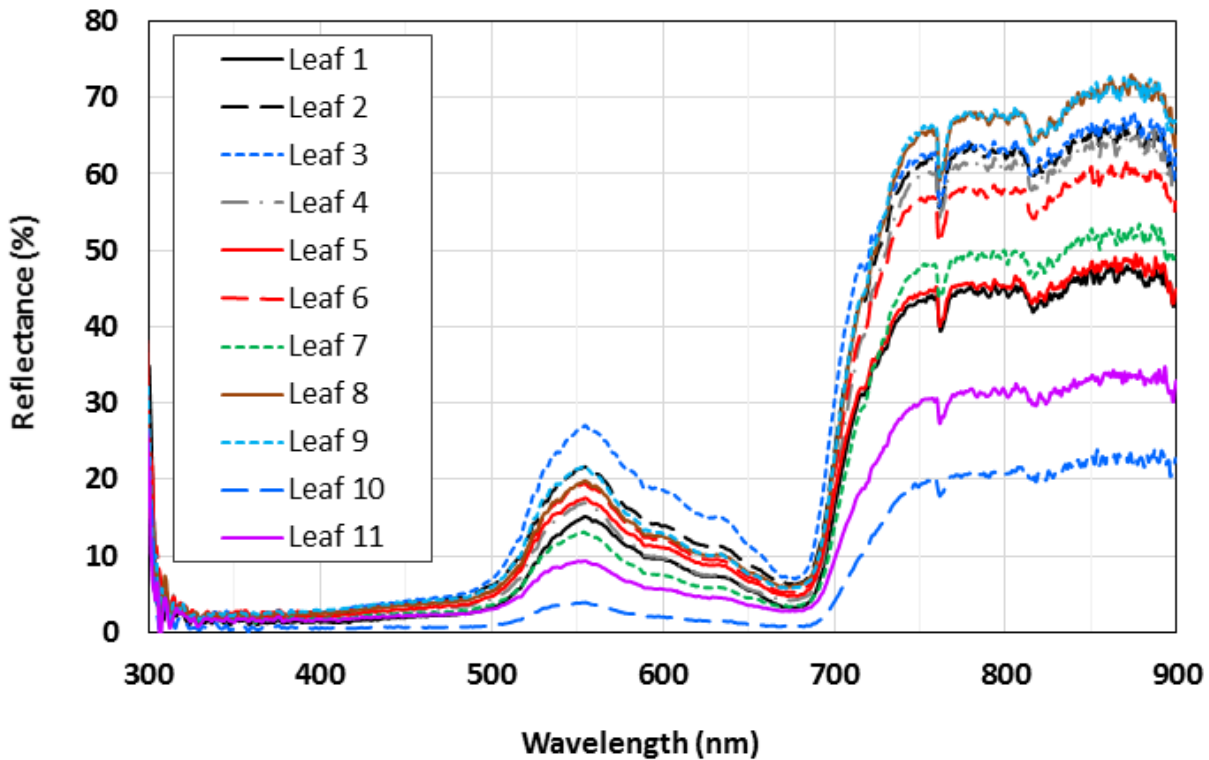
584

585 **4.6. On-site measurement of transmission and reflection spectra of leaves - effect of**  
 586 **leaf orientations**

587 Figure 16 shows leaf-level reflectance measurement on randomly selected leaves on *Tilia*  
 588 1. All the selected leaves were directly and fully illuminated by sunlight, i.e. none of them  
 589 were shadowed in any way. All were tested *in situ* rather than picked off from the tree then

590 tested in the laboratory. The normal of the leaf surface deviated from the sunlight direction  
591 to various extents, and the reflections were measured vertical to the individual leaves. The  
592 reference plane was chosen as vertical to the ground with the same azimuth as that of the  
593 sun.

594



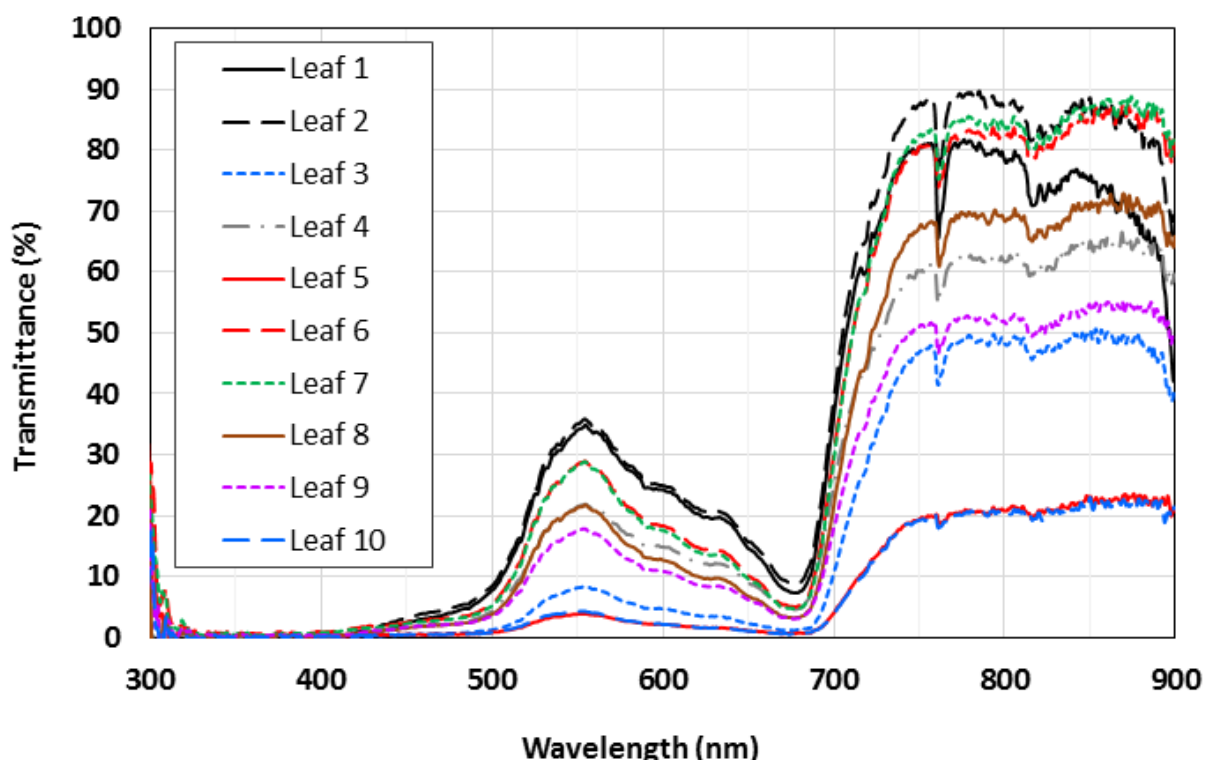
595

596 Figure 16. Leaf-level reflectance measurement on randomly selected leaves which were  
597 fully exposed to sunlight

598

599 Figure 16 shows substantially different reflectance levels of the leaves, from around 20% to  
600 over 60% in the IR regions. The maximum IR reflectance difference was over 40%. This  
601 dramatic difference contrasts with the relatively much smaller levels of reflectance spectra  
602 variation associated with the viewing angles relative to the leaf surface normal in Figure 15.  
603 The principal reason for the dramatic differences seen in Figure 16, is apparently the sun's  
604 angle to the leaf surface, with sunlight more parallel to the leaf surface creating a relatively  
605 less bright leaf surface.

606



607  
608

609 Figure 17. Leaf-level transmittance measurement on randomly selected leaves which were  
610 fully exposed to sunlight

611

612 Figure 17 shows leaf-level transmittance measurement on randomly selected leaves on  
613 *Tilia 1*. All the selected leaves were directly and fully illuminated by sunlight. Dramatic  
614 variations similar to those of on-site leaf-level reflectance were observed, with the maximum  
615 transmittance difference over 60% in the IR region. This is particularly obvious in contrast to  
616 the transmittance spectra which were measured at various viewing angles and much closer  
617 to one another, as seen in Figure 14. The main reason for the substantial differences seen  
618 in Figure 17, as in the case of Figure 16, is apparently the sun's angle to the leaf surface,  
619 with sunlight more parallel to the leaf surface resulting in less solar radiation transmitted  
620 through the leaf. Thus solar position/angles strongly affects both transmission and reflection  
621 of solar radiation through the leaves. As the solar angle changes through the day, insights  
622 presented here reinforce, and offer explanations to, the findings reported in Section 4.3 that  
623 the transfectance spectra measured around a tree crown changes significantly with solar  
624 time.

625

626 The results in Figures 16 and 17 imply that the overall transfectance levels at the crown  
627 level, which are a combination of transmission and reflection of individual leaves, are  
628 significantly affected by the leaf angle distributions within a crown, which may vary with both  
629 tree species and the environmental stress conditions including solar radiation, urban heat

630 and soil water deficit [47]. Crown structure in terms of leaf number, density and angles are  
631 known to change with choice of tree species and with environmental conditions and  
632 stresses, including solar radiation, urban heat, and soil moisture depletion. It follows that  
633 the choice of species and the severity of environmental stress factors will affect crown level  
634 IR solar radiation performance more than performance at the leaf level. In this sense, the  
635 findings have significant implications for species selection and control of environmental  
636 stress factors in urban microclimates.

637

## 638 **5 Conclusions**

639 To study IR radiative performance of urban trees at a crown, rather than leaf, level, new  
640 concepts are necessary to underpin a new framework or methodology. Associated  
641 concepts, including *transflectance (transflection)*, *contributing volume* and *single reference*  
642 *plane* for multiple *patches* of crown surfaces, were introduced and justified here. In the  
643 measurement of tree crown spectroscopy, it was proven that portable miniature  
644 spectrometers suitable for *in situ* tests are valuable in characterising crown level IR  
645 transflection performance despite their often narrower wavelength range. Based on the  
646 methodological framework established here, experimental tests of one type of common tree  
647 species in the UK and Europe, namely lime trees (*Tilia cordata*), have been implemented to  
648 characterise the IR radiative performance of the trees in different scenarios. The main  
649 findings are summarised as follows:

650

- 651 • The reflected and transmitted solar energy from tree leaves is dominated by IR  
652 radiation, which accounts for over 70% of the total reflected or transmitted solar  
653 radiation, respectively.
- 654 • At the leaf level, transmission and reflection spectra are similar (differences typically  
655 < 10% in IR regions) for different trees including those under significantly different  
656 urban stress conditions. In contrast, at the crown level, substantial variations in the  
657 transflectance performance were found between trees. The substantial variations  
658 among transflectance spectra of tree crowns are largely due to crown structural  
659 variations (leaf number, density and angles), rather than the solar interaction  
660 character of the leaves (leaf level transmittance or reflectance, yellower or greener  
661 appearance).
- 662 • Regarding the important factors affecting tree-solar radiation interactions, it is  
663 confirmed that the crown transflectance spectra are affected by viewing angles of the  
664 optical sensor, orientations of measured patches on the tree crown surfaces, local

665 foliage character or non-uniformity of the tree crown structure, as well as the solar  
666 time. For various viewing angles of the optical sensor, the highest IR transfectance  
667 is typically found at the viewing angles deviating from the horizontal. For the  
668 orientation of the measured patches, the transfectance difference between the  
669 maximum and the minimum values in the IR region is about 30% in four cardinal  
670 directions around the crown. Often, but not always (depending on local foliage  
671 characters including leaf density and angles within the FoV of the optical fibre), the  
672 highest values are found in the sunlight direction and lowest on the opposite side.  
673 Also importantly, the crown transfectance spectra change substantially with solar  
674 time in terms of both absolute and relative levels for the various viewing directions.  
675 This change with solar time is particularly pronounced for the four cardinal directions  
676 around a tree crown with a horizontal viewing angle.

- 677 • On-site measurements of transmission and reflection spectra of leaves showed  
678 modest effects of the viewing angle, which resulted in differences of about 10%  
679 among the spectra in the IR region. In contrast, the leaf angle variation created  
680 dramatic spectra differences, with the maximum spectra difference of over 40%  
681 (minimum around 20% and maximum over 60%) in the IR region. It is inferred that  
682 the crown transfectance would be significantly affected by the leaf angle distributions  
683 within the crown.

684

685 These findings have significant implications for species selection and for the control of  
686 environmental stress factors in urban microclimates. We are planning to set up a database  
687 (website) with the infrared radiative performance information of multiple tree species  
688 commonly planted in the UK with different canopy structures as a reference of species  
689 selection for urban planners. Additionally, the new conceptual framework and methodology  
690 presented here will lay a foundation for more comprehensively investigating radiative  
691 interactions among trees, buildings and people.

692

### 693 **Acknowledgement**

694 This work is funded by the UK EPSRC (Grant number: EP/P023819/1).

695

696 **Declaration of interest:** none.

697

698 **References**

- 699 [1] C. Konijnendijk, K. Nilsson, T. B. Randrup, J. Schipperijn, *Urban forests and trees*, Springer-  
700 Verlag Berlin Heidelberg, 2005.
- 701 [2] S. Zheng, J. M. Guldman, Z. Liu, L. Zhao, Influence of trees on the outdoor thermal  
702 environment in subtropical areas: An experimental study in Guangzhou, China, *Sustainable*  
703 *Cities and Society* 42 (2018) 482-497.
- 704 [3] Q. Zhao, D. J. Sailor, E. A. Wentza, Impact of tree locations and arrangements on outdoor  
705 microclimates and human thermal comfort in an urban residential environment, *Urban Forestry*  
706 *& Urban Greening* 32 (2018) 81–91.
- 707 [4] M. A. Irmak, S. Yilmaz, E. Mutlu, H. Yilmaz, Assessment of the effects of different tree species  
708 on urban microclimate, *Environmental Science and Pollution Research* 25 (2018) 15802–  
709 15822.
- 710 [5] L. Kong, K. K. L. Lau, C. Yuan, Y. Chen, Y. Xu, C. Ren, E. Ng, Regulation of outdoor thermal  
711 comfort by trees in Hong Kong, *Sustainable Cities and Society* 31 (2017) 12–25.
- 712 [6] R. Upreti, Z. H. Wang, J. Yang, Radiative shading effect of urban trees on cooling the regional  
713 built environment, *Urban Forestry & Urban Greening* 26 (2017) 18–24.
- 714 [7] S. Gillner, J. Vogt, A. Tharang, S. Dettmann, A. Roloff, Role of street trees in mitigating effects of  
715 heat and drought at highly sealed urban sites, *Landscape and Urban Planning* 143 (2015) 33–  
716 42.
- 717 [8] M. V. Monteiro, T. Blanuša, A. Verhoef, M. Richardson, P. Hadley, R. W. F. Cameron, Functional  
718 green roofs: Importance of plant choice in maximising summertime environmental cooling and  
719 substrate insulation potential, *Energy and Buildings* 141 (2017) 56–68.
- 720 [9] T. Blanus, M. M. V. Monteiro, F. Fantozzi, E. Vysini, Y. Li, R. W. F. Cameron, Alternatives to  
721 Sedum on green roofs: Can broad le  
722 af perennial plants offer better ‘cooling service’, *Building and Environment* 59 (2013) 99–106.
- 723 [10] S. Leuzinger, R. Vogt, C. Koerner, Tree surface temperature in an urban environment,  
724 *Agricultural and Forest Meteorology* 150 (2010) 56–62.
- 725 [11] M. A. Rahman, A. Moser, A. Gold, T. Rötzer, S. Pauleit. Vertical air temperature gradients  
726 under the shade of two contrasting urban tree species during different types of summer days.  
727 *Science of the Total Environment* 633 (2018) 100-111.
- 728 [12] N. J. Georgi and K. Zafiriadis, The impact of park trees on microclimate in urban areas, *Urban*  
729 *Ecosystems* 9 (2006) 195–209.

- 730 [13] M. A. Rahman, A. Moser, T. Rötzer, S. Pauleit. Within canopy temperature differences and  
731 cooling ability of *Tilia cordata* trees grown in urban conditions. *Building and Environment* 114  
732 (2017) 118-128.
- 733 [14] Z. Tan, K. K. L. Lau, E. Ng, Urban tree design approaches for mitigating daytime urban heat  
734 island effects in a high-density urban environment, *Energy and Buildings* 114 (2016) 265–274.
- 735 [15] S. E. Gill, J. F. Handley, A. R. Ennos, S. Pauleit, Adapting cities for climate change: the role of  
736 green infrastructure, *Built Environment* 33 (2007) 115–133.
- 737 [16] AR5 Climate Change 2014: Mitigation of Climate Change — IPCC,  
738 <https://www.ipcc.ch/report/ar5/wg3/>, Accessed date: 10 February 2019.
- 739 [17] J. L. Moss, K. J. Doick, S. Smith, M. Shahrestani, Influence of evaporative cooling by urban  
740 forests on cooling demand in cities, *Urban Forestry & Urban Greening* 37 (2019) 65-73.
- 741 [18] J. Murphy, et al., UK climate projections science report: Climate Change Projections,  
742 Meteorological Office Hadley Centre, Exeter, UK, 2009.
- 743 [19] Shaoni Bhattacharya, European heatwave caused 35,000 deaths, *New Scientists*, Daily News,  
744 2003, <https://www.newscientist.com/article/dn4259-european-heatwave-caused-35000-deaths/>,  
745 Accessed date: 10 February 2019.
- 746 [20] A. Nickson, et al., The Mayor’s climate change adaptation strategy: Managing risks and  
747 increasing resilience, Greater London Authority (GLA), London, 2011.
- 748 [21] L. Zhao, M. Oppenheimer, Q. Zhu, J. W. Baldwin, et al., Interactions between urban heat  
749 islands and heat waves, *Environmental Research Letter* 13 (2018) 034003.
- 750 [22] T. E. Morakinyo, K. K. L. Lau, C. Ren, E. Ng, Performance of Hong Kong’s common trees  
751 species for outdoor temperature regulation, thermal comfort and energy saving, *Building and*  
752 *Environment* 137 (2018) 157–170.
- 753 [23] J. A. Salmond, M. Tadaki, S. Vardoulakis, et al., Health and climate related ecosystem services  
754 provided by street trees in the urban environment, *Environmental Health* 15 (2016) (Suppl  
755 1) :S36.
- 756 [24] M. Rahman, D. Armson, R. Ennos, A Comparison of the Shading Effectiveness of Five Different  
757 Street Tree Species in Manchester, UK, *Journal of Arboriculture* 39 (4) (2013) 157-164.
- 758 [25] M. A. Rahman, D. Armson, A. R. Ennos, A comparison of the growth and cooling effectiveness  
759 of five commonly planted urban tree species, *Urban Ecosyst* 18 (2015) 371–389.



- 760 [26] J. Lindén, P. Fonti, J. Espera, Temporal variations in microclimate cooling induced by urban  
761 trees in Mainz, Germany, *Urban Forestry & Urban Greening* 20 (2016) 198–209.
- 762 [27] M. F. Shahidan, P. J. Jones, J. Gwilliam, E. Salleh, An evaluation of outdoor and building  
763 environment cooling achieved through combination modification of trees with ground materials,  
764 *Building and Environment*, 58 (2012) 245-257.
- 765 [28] T. E. Morakinyo, K. W. D. Kalani. C. Dahanayake, O. B. Adegun, A. A. Balogun, Modelling the  
766 effect of tree-shading on summer indoor and outdoor thermal condition of two similar buildings  
767 in a Nigerian university, *Energy and Buildings* 130 (2016) 721-732.
- 768 [29] Z. H. Wang, X. Zhao, J. Yang, J. Song, Cooling and energy saving potentials of shade trees  
769 and urban lawns in a desert city, *Applied Energy* 161 (2016) 437–444.
- 770 [30] R. Berry, S. J. Livesley, L. Aye, Tree canopy shade impacts on solar irradiance received by  
771 building walls and their surface temperature, *Building and Environment* 69 (2013) 91–100.
- 772 [31] D. Armson, P. Stringer, A. R. Ennos, The effect of tree shade and grass on surface and globe  
773 temperatures in an urban area, *Urban Forestry & Urban Greening* 11 (3) (2012) 245–255.
- 774 [32] V. M. Gómez-Muñoz, M. A. Porta-Gándara, J. L. Fernández, Effect of tree shades in urban  
775 planning in hot-arid climatic regions, *Landscape and Urban Planning*, 94 (3–4) (2010) 149–157.
- 776 [33] B. S. Lin and Y. J. Lin, Cooling Effect of Shade Trees with Different Characteristics in a  
777 Subtropical Urban Park, *HORTSCIENCE* 45(1) (2010) 83–86.
- 778 [34] Z. Tan, K. K. L. Lau, E. Ng, Planning strategies for roadside tree planting and outdoor comfort  
779 enhancement in subtropical high-density urban areas, *Building and Environment* 120 (2017)  
780 93–109.
- 781 [35] T. E. Morakinyo, Y. F. Lam, Simulation study on the impact of tree-configuration, planting  
782 pattern and wind condition on street-canyon's micro-climate and thermal comfort, *Building and*  
783 *Environment* 103 (2016) 262–275.
- 784 [36] R. Kjelgren, T. Montague, Urban tree transpiration over turf and asphalt surfaces, *Atmospheric*  
785 *Environment* 32 (1998) 35–41.
- 786 [37] Reference Solar Spectral Irradiance: ASTM G-173.  
787 <https://rredc.nrel.gov/solar/spectra/am1.5/ASTMG173/ASTMG173.html>, Accessed date: 1 April  
788 2019.
- 789 [38] R. D. Brown, T. J. Gillespie, *Microclimatic landscape design: Creating thermal comfort and*  
790 *energy efficiency*, New York: John Wiley Sons, Inc., 1995.

- 791 [39] T. W. Gara, R. Darvishzadeh, A. K. Skidmore, T. Wang, Impact of vertical canopy position on  
792 leaf spectral properties and traits across multiple species, *Remote Sensing* 10 (2) (2018) 346.
- 793 [40] A. R. Khavaninzadeh, F. Veroustraete, S. Van Wittenberghe, J. Verrelst, R. Samson, Leaf  
794 reflectance variation along a vertical crown gradient of two deciduous tree species in a Belgian  
795 industrial habitat, *Environment Pollution* 201 (2015) 324-332.
- 796 [41] H. M. Noda, T. Motohka, K. Murakami, H. Muraoka, K. N. Nasahara, Reflectance and  
797 transmittance spectra of leaves and shoots of 22 vascular plant species and reflectance spectra  
798 of trunks and branches of 12 tree species in Japan, *Ecological Research* 29 (2) (2014) 111–  
799 123.
- 800 [42] S. P. Serbin, D. N. Dillaway, E. L. Kruger, P. A. Townsend, Leaf optical properties reflect  
801 variation in photosynthetic metabolism and its sensitivity to temperature, *Journal of*  
802 *Experimental Botany* 63 (2012) 489–502.
- 803 [43] W. Henrion and H. Tributsch, Optical solar adaptations & radiative temperature control of green  
804 leaves and tree barks, *Solar Energy Materials and Solar Cells* 93 (2009) 98–107.
- 805 [44] E. J. Milton, G. A. Blackburn, E. M. Rollin, F. M. Danson, Measurement of the spectral  
806 directional reflectance of forest canopies: A review of methods and a practical application,  
807 *Remote Sensing Reviews* 10 (4) (1994) 285–308.
- 808 [45] D. A. Roberts, S. L. Ustin, S. Ogunjemiyo, et al., Spectral and Structural Measures of Northwest  
809 Forest Vegetation at Leaf to Landscape Scales, *Ecosystems* 7 (5) (2004) 545–562.
- 810 [46] D. S. Kimes, (1983) Dynamics of directional reflectance factor distributions for vegetation  
811 canopies, *Applied Optics* 22 (9) (1983) 1364-1372.
- 812 [47] D. S. Falster and M. Westoby, Leaf size and angle vary widely across species: what  
813 consequences for light interception? *New Phytologist* 158 (3) (2003) 509–525.

814

815

816

817 **Figure Captions:**

818

819 Figure 1. Tree crown-level interactions with solar radiation, illustrating the concepts of  
820 transfectance (transflection) for a patch being measured; FOV=Field of View

821 Figure 2. An illustration of a tree model (model 1) showing azimuth and altitude angles and  
822 reference plane location for a specific patch of crown surface

823 Figure 3. An illustration of solar azimuth and altitude angles in relation to a tree being  
824 studied

825 Figure 4. An illustration of a patch of crown surface showing azimuth and altitude angles for  
826 the spectrometer optical fibre

827 Figure 5. An illustration of tree model 2 and contributing volume

828 Figure 6. Test site and *Tilia* trees (a) 3-9, (b) 1 and a tripod holding a spectrometer, sampling  
829 fibre and laptop, (c) 1 in foreground, 2 to the right, (d) 7-9 (right to left)

830 Figure 7. Schematic showing location of the 10 *Tilia cordata* trees

831 Figure 8. Samples of the reflected irradiance spectrum from a leaf on *Tilia* 7 and the  
832 transmitted irradiance spectrum from a leaf on *Tilia* 1

833 Figure 9. Leaf reflectance spectra of *Tilia* 10, *Tilia* 7 and *Tilia* 1 in question

834 Figure 10. *Tilia* 1 transflectance measurement – effect of viewing angles of the optical fibre  
835 in a vertical plane

836 Figure 11. *Tilia* 1 transflectance measurement – spectra measured in four cardinal  
837 directions around the tree during 9:45–10:45 am BST

838 Figure 12. *Tilia* 1 transflectance measurement – spectra measured in four directions around  
839 the tree at 2 pm BST

840 Figure 13. Transflectance spectra of all 10 *Tilia* trees

841 Figure 14. Leaf transmission spectra measured from various viewing angles

842 Figure 15. Leaf reflection spectra measured from various viewing angles

843 Figure 16. Leaf-level reflectance measurement on randomly selected leaves which were  
844 fully exposed to sunlight

845 Figure 17. Leaf-level transmittance measurement on randomly selected leaves which were  
846 fully exposed to sunlight